character. For this reason this source is only likely to be identified experimentally in static tests when microphones are placed close to the appropriate Mach wave propagation angle. However, on a flyover there will be a period when the levels on the flight path may be dominated by this type of highly directional source.

Acknowledgment

This work was supported by Nasa Research Grant NAG-1-715. The author would like to thank Dr. F. Farassat for his assistance.

References

[1]Glegg, S., "Significance of Unsteady Thickness Noise," *AIAA Journal*, Vol. 23, 1987, pp. 839-844.

[2]Amiet, R. K., "Acoustic Radiation from an Airfoil in a Turbulent Stream," *Journal of Sound and Vibration,* Vol. 41, 1975, pp. 407-420.

[3]Mugridge, B. D. and Morfey, C. L., "Sources of Noise in Axial Flow Fans," *Journal of the Acoustical Society of America,* Vol. 51, 1972, pp. 1411-1426.

[4]Sevik, M., "Sound Radiation from a Subsonic Rotor Subjected to Turbulence," NASA SO-304, Part II, 1970.

Spectral Measurements of Pressure Fluctuations on Riblets

W. L. Keith*
Naval Underwater Systems Center, New London, Connecticut

Introduction and Experimental Apparatus

A RECENT summary of riblet research is given by Wilkinson et al.[1] of NASA Langley. The authors state, "Of all the nonplanar surface approaches to turbulent viscous drag reduction, riblets are the best established, with little, if any, remaining doubt regarding their effectiveness. The main thrust of the initial Langley riblet research was to verify riblet drag reduction and optimize its level. This effort culminated in the selection of a symmetrical V-groove as the optimal design ($h^+ = S^+ = 15.8$ percent drag reduction)." The investigation reported here was aimed at determining if any measurable changes are induced by riblets in the autospectral density, the streamwise cross-spectral density, and the convection velocity of the fluctuating wall pressure field. Due to the attenuation resulting from spatial averaging, only scales associated with the outer region of the turbulent boundary layer were resolved.

The experiments were conducted in the rectangular test section of the quiet water tunnel at the Naval Underwater Systems Center, New London Laboratory. The water tunnel is a recirculating flow facility, with acoustic isolation provided by rubber hoses between the test section, plenum chambers, and centrifugal pump. The interior of the test section is 83 in. long, 12 in. wide, and increases in height linearly from 4 in. at the inlet to 4.41 in. at the exit, resulting in a zero pressure gradient flow to within ±0.005 psi. Two piezoelectric pressure transducers fabricated of PZT-5H Type 2 material, of diameter 0.08 in., were flush mounted in the bottom wall, with a streamwise separation of 0.4 in. center to center. The output voltage signals were amplified 20 dB by an Ithaco Model 143N preamplifier, an additional 20 dB by an Ithaco Model 455 amplifier with an adjustable high pass filter (set at 1 Hz), and were then input to a Spectral Dynamics Model SD375 spectrum analyzer. All of the spectra were computed from 500 ensemble averages. Measurements of the mean streamwise velocity $u(y)$ were made using a TSI model 9100 laser Doppler velocimetry system. The riblet coating, which was identical to that used on the yacht "Stars and Stripes," was manufactured by the Scotch 3M Corporation. The symmetrical V-grooves had height (h) and peak-to-peak spacings (S) of 0.0045 in., and a base thickness of 0.0025 in. Following the baseline measurements, the entire bottom wall of the rectangular test section was covered with one continuous layer of riblet material. The riblets extended a distance upstream approximately 60 δ from the measurement location.

Experimental Results

The turbulent boundary-layer mean velocity profiles were measured at a streamwise location coincident with that of the pressure transducers, 61.4 in. from the test section inlet and 6 in. from each side wall. The displacement thickness δ^* and momentum thickness θ, determined by numerical integration, are given in Table 1. Based on the R_θ values and velocity profiles, a fully developed turbulent boundary layer existed at both Reynolds numbers. The turbulence intensity in the freestream was 1.5%. In order to determine the mean wall shear stress τ_ω, the boundary-layer profiles and static pressures were measured at streamwise locations along the test section. Values for τ_ω were then determined from a momentum balance analysis. The velocity defect $[(U_\infty - u(y)]/u^*$ was plotted for both Reynolds numbers investigated and was found to agree well with Hama's[2] empirical expression for zero pressure gradient flat-plate turbulent boundary layers, given as $9.6(1-y/\delta)^2$. The nondimensional scales of the riblets S^+ and pressure transducers d^+ are given in Table 1. The freestream velocity of 10 ft/s provided an optimum turbulent boundary layer for the performance of the riblets, based on the results of Wilkinson et al.[1]

Corcos[3] derived a method to correct autospectra for the attenuation due to spatial averaging associated with circular-faced transducers. The baseline measurements of the corrected autospectral density $\Phi(\omega)$ nondimensionalized on outer flow variables δ^* and U_∞ are presented in Fig. 1. Also shown are the

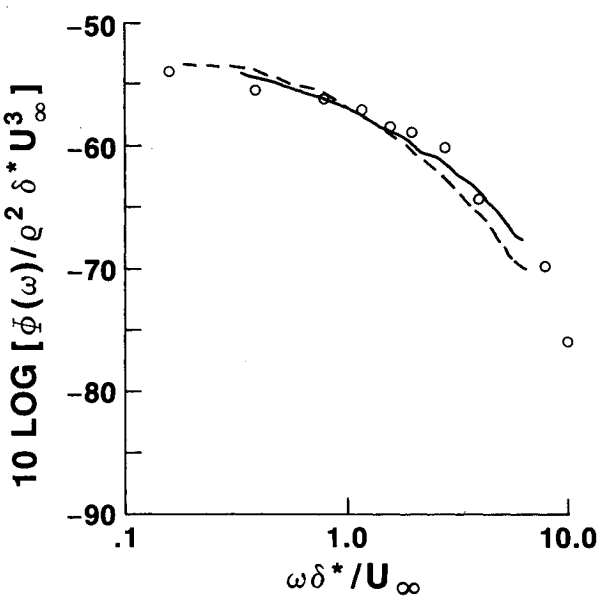

Fig. 1 Nondimensional autospectra $\Phi(\omega)/\rho^2\delta^* U_\infty^3$. Corrected for spatial averaging, — $U_\infty = 10$ (ft/s), --- $U_\infty = 20$ (ft/s), o = results of Bakewell et al.[4]

Received Sept. 16, 1988; revision received Feb. 28, 1989.

*Submarine Sonar Department.

Table 1 Turbulent boundary-layer parameters and inner scales

U_∞ (ft/s)	δ (in.)	δ^* (in.)	θ (in.)	R_θ	ν/u^* (in.)	$S^+ = Su^*/\nu$	$d^+ = du^*/\nu$
10	1.14	0.17	0.12	1.00×10^4	3.2×10^{-4}	14.1	250.0
20	1.01	0.14	0.11	1.83×10^4	1.5×10^{-4}	30.0	533.3

Table 2 Comparison of parameters with Bakewell et al.[4]

	U_∞ (ft/s)	δ (in.)	R_δ	d/δ^*	p_{rms}/q	p_{rms}/q corrected
Bakewell (air)	178	1.75	1.50×10^5	0.04	4.60×10^{-3}	4.90×10^{-3}
Present investigation (water)	10	1.14	0.95×10^5	0.07	3.95×10^{-3}	4.85×10^{-3}
	20	1.01	1.68×10^5	0.08	3.90×10^{-3}	4.69×10^{-3}

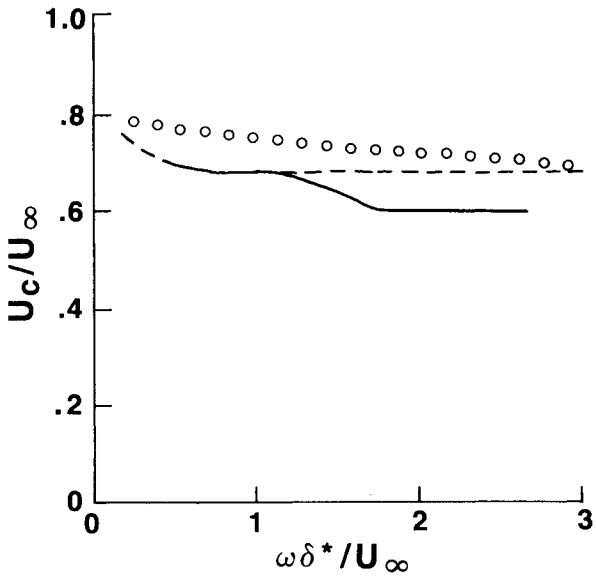

Fig. 2 Nondimensional convection velocity U_c/U_∞, — $U_\infty = 10$ (ft/s), --- $U_\infty = 20$ (ft/s), o = results of Willmarth.[6]

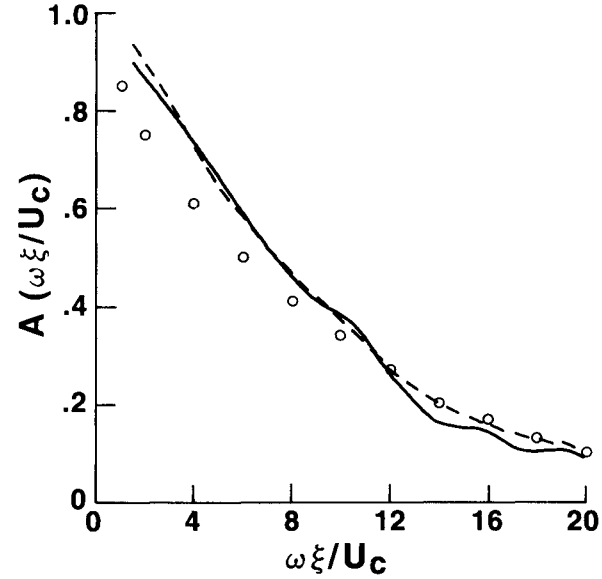

Fig. 3 Normalized longitudinal cross-spectral density $A(\omega\xi/U_c)$, $U_\infty = 10$ (ft/s), — = baseline, --- = riblets, o = results of Willmarth.[6]

corrected measurements of Bakewell et al.,[4] which were made in a fully developed turbulent pipe flow of air. The mean square of the fluctuating pressure $p(t)$ may be expressed as

$$\overline{p(t)^2} = \int_0^\infty \Phi(\omega)\, d\omega$$

where $\Phi(\omega)$ is the single-sided autospectral density of the pressure fluctuations. The root-mean-square pressure coefficient p_{rms}/q, where $p_{rms} = \overline{p(t)^2}^{1/2}$ and $q = \rho U_\infty^2/2$, was determined at each Reynolds number by subtracting the background noise from the measured autospectra and integrating over the non-dimensional frequency range $0.18 < \omega\delta^*/U_\infty < 6.23$. Table 2 contains a comparison of both the corrected and uncorrected values of p_{rms}/q for this investigation with those of Bakewell et al. The frequency range for Bakewell et al. was $0.14 < \omega\delta^*/U_\infty < 9.87$.

Corcos[3] proposed the following model for the longitudinal cross-spectral density function $\Phi_{x\xi}(\omega)$:

$$\Phi_{x\xi}(\omega) = \Phi(\omega) A\left(\frac{\omega\xi}{U_c}\right) e^{-i\omega\xi/U_c}$$

where $\omega\xi/U_c$ is a similarity variable with ξ the separation between the two streamwise measurement locations, and U_c the convection velocity of the pressure-producing eddies. From this relationship, the function $A(\omega\xi/U_c)$ may be defined as the magnitude of the normalized longitudinal cross-spectral density. Following Smol'yakov and Tkachenko,[5] the convection velocity was found from the phase $\phi(\omega)$ of the cross-spectral density function $\Phi_{x\xi}(\omega)$, where $U_c = \omega\xi/\phi(\omega)$. The quantity U_c/U_∞ is presented as a function of $\omega\delta^*/U_\infty$ in Fig. 2 for both Reynolds numbers, along with Willmarth's[6] results. The functions $A(\omega\xi/U_c)$ are shown in Figs. 3 and 4. The experimental error in the magnitude of $A(\omega\xi/U_c)$ is ± 0.01. Corcos[3] has estimated the correction in the measurement of the cross-spectral density for spatial averaging to be small compared to that for the autospectra.

All of the measurements were repeated with the riblet coating installed. The presence of an elastomeric coating above a pressure transducer causes an attenuation of the convected high wave number pressure disturbances. Previous measurements, made with the same type of transducer mounted such that 0.031 in. of urethane covered the face, showed a maximum attenuation of approximately 5 dB in $\Phi(f)$ at the highest frequencies measured at each Reynolds number. If we assume an average thickness for the riblet material of 0.005 in., the maximum attenuation at the highest frequencies measured here is less than 1 dB.

The autospectra $\Phi(f)$ measured beneath the riblet coating are shown in Figs. 5 and 6 along with the baseline measurements. No significant change was measured for either of the Reynolds numbers. The small reductions at the highest and lowest measured frequencies at $U_\infty = 10$ ft/s are attributable to slight variations in the background noise. At frequencies greater than 100 Hz, the background noise was electronic, and below 100 Hz the source was acoustic waves generated by the centrifugal pump and transmitted by the working fluid. The

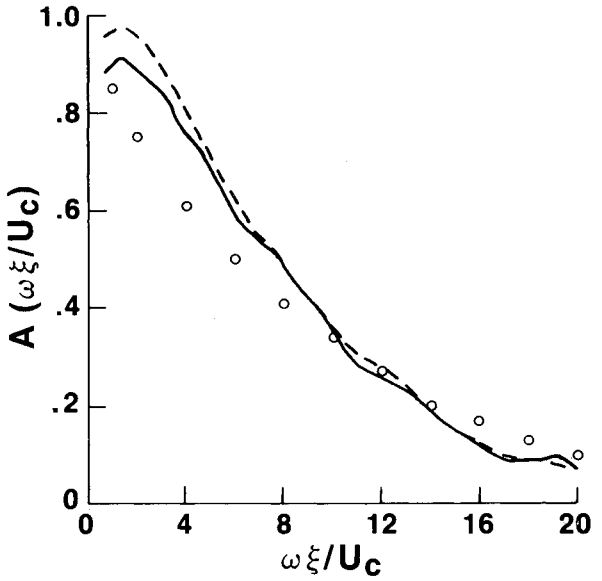

Fig. 4 Normalized longitudinal cross-spectral density $A(\omega\xi/U_c)$, $U_\infty = 20$ (ft/s), — = baseline, --- = riblets, o = results of Willmarth.[6]

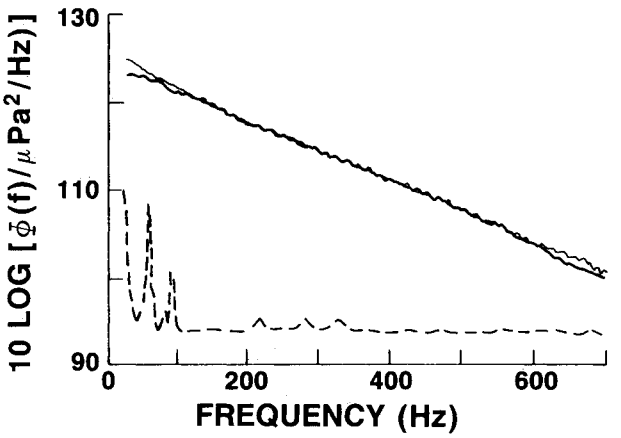

Fig. 5 Autospectral density $\Phi(f)$, $U_\infty = 10$ (ft/s), — = baseline, ▬ = riblets, --- = background noise.

spectra in Figs. 5 and 6 have not been corrected for spatial averaging. For the case of $R_\theta = 1.0 \times 10^4$, the attenuation (based on Corcos' correction) was 4.1 dB at 350 Hz and 10.7 dB at 700 Hz. For $R_\theta = 1.8 \times 10^4$, the attenuation was 4.1 dB at 800 Hz and 11.0 dB at 1600 Hz. The measured convection velocities were identical to within ±0.5% with those of the baseline measurements, shown in Fig. 2. A small but measureable increase in the magnitude of $A(\omega\xi/U_c)$ occurred at low values of $\omega\xi/U_c$, as shown in Figs. 3 and 4, with the effect being greater at the higher Reynolds number. Blake[7] measured a broadband decrease in the magnitude of $A(\omega\xi/U_c)$, a decrease in the convection velocities, and an increase in $\Phi(\omega)$ due to roughness elements, with heights on the order of 150 to 300 viscous lengths. He concluded that correlation distances were significantly reduced, due to the roughness elements. Blake's measurements qualitatively suggest that a reduction in drag due to skin friction would accompany an increase in the magnitude of $A(\omega\xi/U_c)$, as measured here. A limitation of this investigation is the lack of resolution of convected wave numbers with scales associated with the wall region of the turbulent boundary layer. Riblets may induce changes in these wave numbers that lead to changes in the levels of the autospectra at the associated frequencies. The results presented here show that the net contribution to the autospectra as well as the convection velocities from wave numbers associated with the outer region of the turbulent boundary layer is not significantly changed by the presence of riblets.

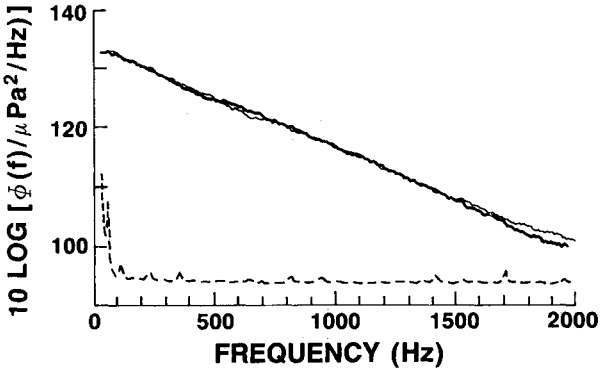

Fig. 6 Autospectral density $\Phi(f)$, $U_\infty = 20$ (ft/s), — = baseline, ▬ = riblets, --- = background noise.

Acknowledgments

Funding for this investigation was provided by the Naval Underwater Systems Center IR/IED Program, Job Order A70260. The author is grateful to Professor W. Willmarth at the University of Michigan for many helpful suggestions.

References

[1]Wilkinson, S. P., Anders, J. B., Lazos, B. S., and Bushnell, D. M., "Turbulent Drag Research at NASA Langley—Progress and Plans," *Proceedings of the Royal Aeronautical Society, Turbulent Drag Reduction by Passive Means,* London, Sept. 1987, pp. 1-32.

[2]Hama, F. R., *Society of Naval Architects Marine Engineers Transactions,* Vol. 62, 1954, p. 333-358.

[3]Corcos, G. M., "Resolution of Pressure in Turbulence," *Journal of the Acoustical Society of America,* Vol. 35, Feb. 1963, pp. 192-199.

[4]Bakewell, H. P., Jr., Carey, G. F., Schloemer, H. H., and Von Winkle, W. A., "Wall Pressure Correlations in Turbulent Pipe Flow," USL Rept. No. 559, 1-052-00-00, Naval Underwater Systems Ctr., New London, CT, 1962.

[5]Smol'yakov, A. V. and Tkachenko, V. M., *The Measurement of Turbulent Fluctuations,* Springer-Verlag, New York, 1983, pp. 32-35.

[6]Willmarth, W. W., "Pressure Fluctuations Beneath Turbulent Boundary Layers," *Annual Review of Fluid Mechanics,* Vol. 7, 1975, pp. 13-39.

[7]Blake, W. K., "Aero-Hydroacoustics for Ships," DTNSRDC-84/010, U.S. Government, Dept. of the Navy, Bethesda, MD, Vol. 2, 1984.

Calculation of Asymmetric Vortex Separation on Cones and Tangent Ogives Based on a Discrete Vortex Model

Suei Chin* and C. Edward Lan†
University of Kansas, Lawrence, Kansas
and
Thomas G. Gainer‡
NASA Langley Research Center, Hampton, Virginia

Introduction

DISCRETE line vortices have been used in the past to model symmetric[1,2] and asymmetric[3] vortx separations at zero sideslip in the leeward side of a body. In these

Received Sept. 26, 1988; revision received April 7, 1989.

*Graduate Research Assistant. Student Member AIAA.

†Professor, Department of Aerospace Engineering. Associate Fellow AIAA.

‡Aerospace Engineer.